Available online at www.sciencedirect.com
ScienceDirect
Journal of the European Ceramic Society 29 (2009) 2951–2957
www.elsevier.com/locate/jeurceramsoc

Microwave-assisted synthesis of Pr–$ZrSiO_4$, V–$ZrSiO_4$ and Cr–$YAlO_3$ ceramic pigments

M. Blosi [a,b], M. Dondi [b,*], S. Albonetti [a], G. Baldi [c], A. Barzanti [c], C. Zanelli [b]

[a] *Department of Industrial and Materials Chemistry, University of Bologna, Viale Risorgimento 4, 40136 Bologna, Italy*
[b] *ISTEC-CNR, Institute of Science and Technology for Ceramics, Via Granarolo 64, 48018 Faenza, Italy*
[c] *CE.RI.COL., Colorobbia Research Centre, Via Pietramarina 123, 50053 Sovigliana-Vinci, Italy*

Received 15 January 2009; received in revised form 6 April 2009; accepted 16 April 2009
Available online 30 May 2009

Abstract

An innovative two-step route was successfully applied to the microwave-assisted synthesis of Pr–$ZrSiO_4$, V–$ZrSiO_4$ and Cr–$YAlO_3$ ceramic pigments. It is able to reduce the total synthesis time from many hours down to a few minutes. Industrial batches were pelletized and underwent a short time pre-heating in conventional electric furnace (from 300 up to 1000 °C) prior to dielectric heating in microwave oven (2.45 GHz, 800 W continuous or paused). Pre-heating is necessary to reach a thermal level at which pigment precursors are activated under microwave irradiation (high enough tan δ of dielectric properties). Activation kinetics was followed by measuring (optical pyrometer) the external temperature of crucible during MW irradiation and the internal temperature at the end of heating process. Pigments were characterized by colourimetry (CIE Lab) and XRPD with Rietveld refinement. The V–$ZrSiO_4$ system is easily activated, already at pre-heating of 300 °C, with good reaction yield and colour performance; nevertheless it is difficult to keep under control, as temperatures exceeding 1200 °C are rapidly reached. The Pr–$ZrSiO_4$ system is activated after pre-heating over 600 °C and exhibits a slow kinetics, resulting in a low reaction yield and unsatisfactory colour. The Cr–$YAlO_3$ pigment is formed with colour and reaction yield close to those of the correspondent industrial product, even though after pre-heating at 800 °C or more. A peculiar behaviour of silica phases was observed in zircon systems, particularly after lower pre-heating temperatures. It consists in an early transformation of quartz (present as precursor) into cristobalite and abundant amorphous phase, before the $SiO_2 + ZrO_2 \rightarrow ZrSiO_4$ transformation occurred.

Keywords: A. Microwave processing; B. X-ray methods; C. Optical properties; D. Perovskites; Ceramic pigment

1. Introduction

The microwave-assisted synthesis is a promising way to improve the conventional heating process used to get oxidic structures, accelerating kinetics of solid state reactions.[1] Microwave heating was successfully applied in the solid state synthesis of several oxides of transition metals: Co–Fe, Ni–Fe and Fe–Fe spinels,[2–4] Cr_2O_3 and Fe_2O_3,[4–6] yttrium iron garnet YIG[7] and (La,Sr,Ca)XO_3 perovskites, where X is Cr,[8,9] Co and Fe[10,11] or Mn.[3]

In recent times, microwaves are being widely utilized to synthesize oxide nanoparticles and also nanoporous or nanostructured materials by dielectric heating of solutions[12–14] often in hydrothermal conditions.[15–19] At any rate, this route has at the moment little appeal for large-scale production of colorants, so it is not considered in this study.

In the field of ceramic pigments, Bondioli et al. did a pioneering work succeeding in the MW-assisted solid state synthesis of Al_2O_3–Cr_2O_3 and CeO_2:Pr.[5,19,20] A further step was recently done by obtaining black $CoFe_2O_4$ and coral-red $ZrSiO_4$:Fe_2O_3 pigments, although the MW heating was not fully successful for the Al_2O_3:Mn and SnO_2:Cr systems.[21] These results are somewhat expected, since the main hindrance to the MW application in solid state synthesis consists in having into the system at least one component with suitable dielectric properties, particularly a large enough tangent loss: $\tan\delta = \varepsilon''/\varepsilon'$, where ε'' is the dielectric loss and ε' is the dielectric constant.[22,23] This occurs with pigments containing a significant amount of transition metals, which are sensitive to MW irradiation (i.e. have high values of $\tan\delta$) already at room temperature, so transfer heat to the other

* Corresponding author.
E-mail address: dondi@istec.cnr.it (M. Dondi).

0955-2219/$ – see front matter © 2009 Published by Elsevier Ltd.
doi:10.1016/j.jeurceramsoc.2009.04.022

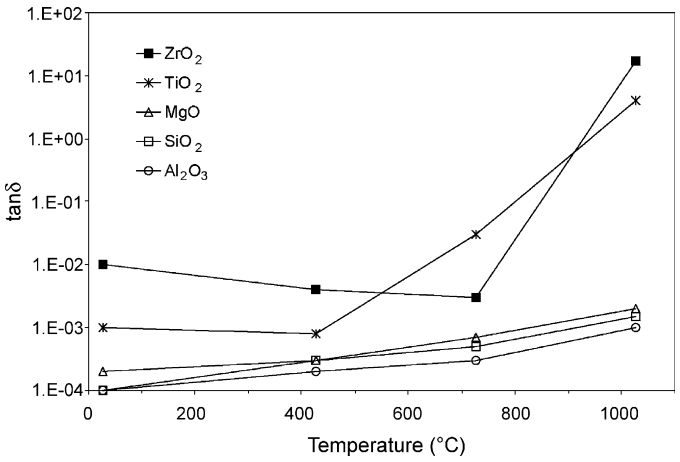

Fig. 1. Tangent loss versus temperature of binary oxides.[23]

components, which are transparent to microwaves.[20,21] When the content of transition metals is low, as in allochromatic pigments, there is no significant dielectric heating of precursors and direct synthesis of very important ceramic stains, like those based on zircon or aluminates, is not viable.

However, some compounds turn to be MW-active during the thermal treatment, as their tangent loss has a marked dependence on temperature, as the case of ZrO_2, which $\tan\delta$ values increase fastly over a certain activation temperature T_a (Fig. 1). This behaviour has been exploited in the present research, whose main goal is to synthesize allochromatic pigments by solid state reaction through an innovative two-step procedure: rapid heating in conventional furnace to trespass T_a then fast synthesis in MW oven. Three systems were taken into consideration, corresponding to important ceramic pigments: yellow praseodymium-doped $ZrSiO_4$,[24,25] turquoise vanadium-doped $ZrSiO_4$[26,27] and red chromium-doped $YAlO_3$.[28,29] The rationale was studying first the activation temperature of each system, then performing the two-step synthesis procedure at the proper temperature, determining reaction yield and colour performance by quantitative XRPD and colourimetry, respectively, and eventually comparing data with industrial pigments, synthesized by the conventional ceramic route, taken as benchmark.

2. Experimental

Three systems were taken into consideration: Cr:$YAlO_3$ (YC), Pr:$ZrSiO_4$ (ZP), and V:$ZrSiO_4$ (ZV), using industrial formulations. Batches contained precursors (Al_2O_3, SiO_2, Y_2O_3, ZrO_2) in stoichiometric amounts, dopants (1.1 wt.% Cr, 1.7 wt.% Pr, 2.5 wt.% V, all added as oxides) and mineralizers (NaF, NaCl, CaF_2, $BaCl_2$; total amount is 4 wt.% in YC and ZP, 8 wt.% in ZV) and were admixed in the manufacturing plant.

Samples were pelletized by adding a drop of a PEG 400 water solution (3 wt.%) to 5 g of powder and uniaxial pressing (50 MPa) of cylinders (10 mm diameter and 5 mm height). Every dry pellet was put into a bubble alumina crucible, containing corundum (in the case of YC) or zircon sand (for ZP and ZV), being all these materials transparent to microwaves.

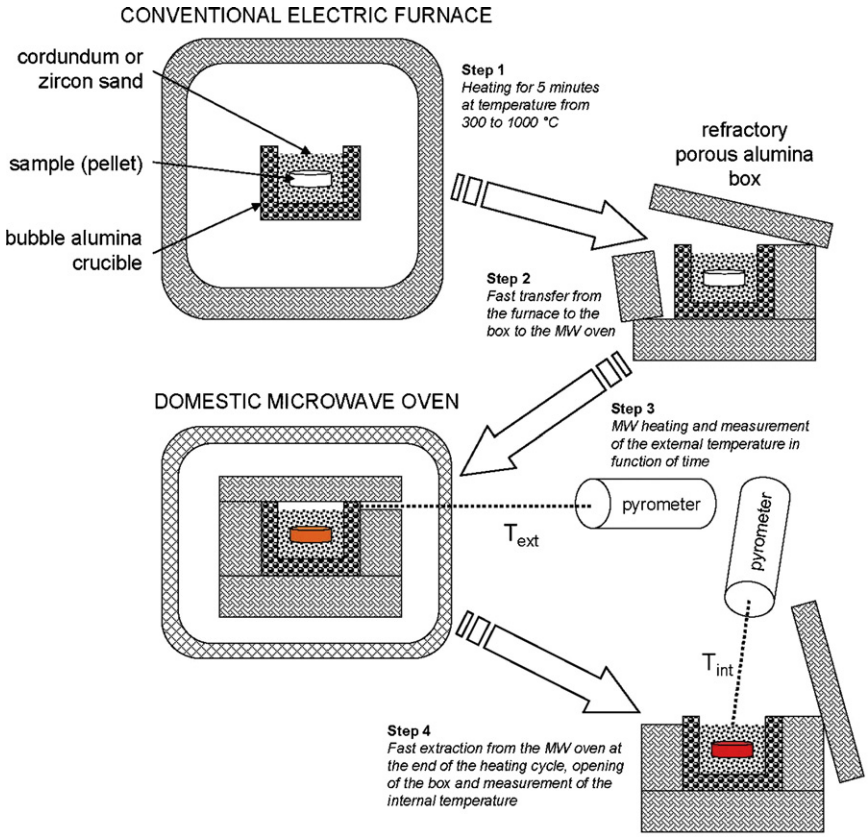

Fig. 2. Sketch of the synthesis procedure and temperature measurements.

The MW-assisted synthesis was carried out by an innovative two-step route:

(1) Activation by pre-heating in conventional electric furnace, putting the sample directly at a temperature variable in the 300–1000 °C range, then soaking for 5 min. Extraction from the electric furnace, allocation into an alumina refractory box (Fig. 2) and fast transfer to the MW oven. This operation implied a decrease from 50 to 100 °C of the actual temperature of the crucible, depending on the pre-heating temperature of furnace, which was accordingly set up to a higher temperature, in order to overcome this drawback.
(2) Dielectric heating by a domestic MW oven (DeLonghi, 2.45 GHz) with different power curves: 800 W implies continuous MW irradiation at full power (800 W); 560 W means 20 s full power and 10 s pause; 400 W stands for 20 s full power and 20 s pause.

The kinetics of activation was investigated by measuring the temperature of crucible in function of time by means of an optical pyrometer (Minolta Cyclops 52, emissivity 0.3 for alumina, 0.7 for dark-coloured zircon sand, experimental uncertainty ±20 °C). The external temperature (T_{ext}) was measured during the MW heating focussing on the external wall of crucible inside the MW oven (Fig. 2). The internal temperature (T_{int}) was measured at the end of each heating cycle, removing the lid of refractory box and focussing on the top of the corundum or zircon filling of crucible. In order to get the T_{int} curve, the T_{ext} versus time curve was corrected by a factor $\Delta T = T_{int} - T_{ext}$.

X-ray powder diffraction (XRPD, Rigaku Geigerflex, 10–80° 2θ, 0.02°/s, 5 s per step) was used to determine the reaction yield (i.e. weight percent of the desired pigment) by quantitative phase analysis as well as the unit cell parameters of zircon and perovskite. The Rietveld full profile refinement was performed using the GSAS-EXPGUI softwares,[30,31] achieving quantitative data with an experimental uncertainty of about 0.5%. The main agreement indices as defined in GSAS for the final least-squares cycles are represented by R_p (%), R_{wp} (%) and RF^2 (%). For ZP and ZV samples the agreement indices ranges are: $5.3\% < R_p < 11.3\%$, $7.9\% < R_{wp} < 15.3$ and $3.5 < RF^2 < 16.4$, while for YC they are $15.5\% < R_p < 18.4\%$, $19.5\% < R_{wp} < 23.3$ and $7.4 < RF^2 < 10.0$. Rietveld results of ZP and ZV samples were normalized to a constant ZrO_2 content and the difference to 100% was estimated to be the amount of amorphous phase. The XRPD analyses were carried out on samples taken from the MW oven, quenched in air and ground in agate mortar to a particle size passing the 50 μm sieve. The duration time of MW treatment was 5 min for all samples of the systems YC and ZP. Due to very fast heating rate, the ZV samples underwent decreasing times of MW irradiation, in order to prevent overfiring and crucible melting, for the different pre-heating temperatures: 300–500 °C (5 min), 600–800 °C (3 min), and 1000 °C (1 min).

The colour performance was measured on the quenched and pulverized samples by diffuse reflectance spectroscopy (HunterLab Miniscan MSXP4000, 400–700 nm, D_{65} standard illuminant, 10° observer, white glazed tile reference $x = 31.5$, $y = 33.3$) and expressed as CIE-Lab coordinates: L^* (100 = white, 0 = black), a^* (+red, −green), and b^* (+yellow, −blue). Results are expressed as colour performance (CP), which was calculated as:

$$CP = \frac{b^*_{MW}}{b^*_{ind}} \times 100 \quad \text{(for the systems ZP and ZV)},$$

$$CP = \frac{a^*_{MW}}{a^*_{ind}} \times 100 \quad \text{(for the system YC)},$$

where the subscript "MW" indicates the pigment synthesized by dielectric heating, while the subscript "ind" indicates the reference pigment, obtained with the same batch by conventional heating in the industrial furnace.

3. Results and discussion

The systems under investigation exhibit a different aptitude to dielectric heating, as each pigment is activated starting from its own pre-heating temperature, which is increasing from V–$ZrSiO_4$ (∼300 °C) to Pr–$ZrSiO_4$ (∼600 °C) to Cr–$YAlO_3$ (∼700 °C). This different behaviour is appreciable also by the activation kinetics measured as increase of temperature during microwave irradiation (Fig. 3). Account must be taken that the temperature attained under MW irradiation depends on the pre-heating treatment: the higher the temperature of electric furnace, the faster the heating kinetics due to microwaves.

The batch of turquoise pigment ZV is readily activated: the external temperature of crucible increases fastly, reaching 1000 °C after 3 min at full power, and temperatures over 700 °C even with paused irradiation, i.e. 560 or 400 W (Fig. 3). The yellow pigment ZP presents a slower kinetics of microwave activation: it takes more time to show a first significant heating, beyond that the external temperature grows slowly to 900 °C (800 W) or fluctuates around 700 °C (560 W) or 600 °C (400 W). The YC perovskite is activated only under full power, although with a slow kinetics, attaining 750 °C at the external wall of crucible after 6 min of MW irradiation.

In any case, the actual temperatures at the interior of crucible are significantly higher than those measured at the external wall and an estimation is given in Fig. 4. The pigment ZV increases rapidly its temperature, reaching 1200 °C in 3 min at full power (or 5 min in the paused schedule). This behaviour is probably due to the combined effect of ZrO_2 precursor, which increases fastly its $\tan\delta$ over 700 °C (Fig. 1), and the relatively high amount of transition metal contained (2.5 wt.% V) which likely acted as MW absorber. In contrast, both the ZP and YC pigments reach at maximum 1000 °C under full power; using the paused MW irradiation, YC is not activated, while ZP exhibit a very slow kinetics. The behaviour of the ZP batch is presumably governed by the $ZrO_2 + SiO_2 \rightarrow ZrSiO_4$ transformation, being the very low amount of transition metal oxide (1.7 wt.% Pr) probably non-influent. Even if the $\tan\delta$ versus temperature curve of zircon is not known, it is likely that ZrO_2 be the only component of the ZP batch susceptible to MW at high temperature. It may be envisaged a dynamic process where the dielectric heating is ensured by zirconia only, which absorbing microwaves

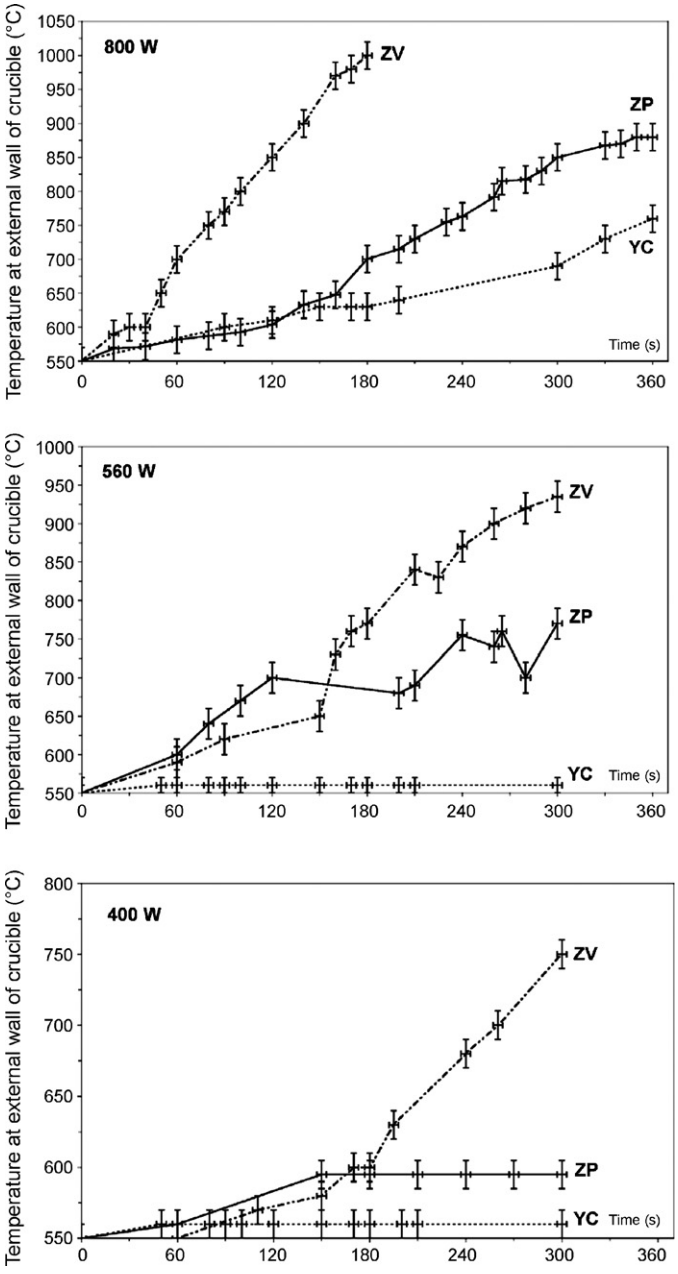

Fig. 3. Activation kinetics of the Cr:$YAlO_3$ (YC), Pr:$ZrSiO_4$ (ZP), and V:$ZrSiO_4$ (ZV) systems: temperature at external wall of crucible in function of time at different MW power (pre-heating temperature: 700 °C).

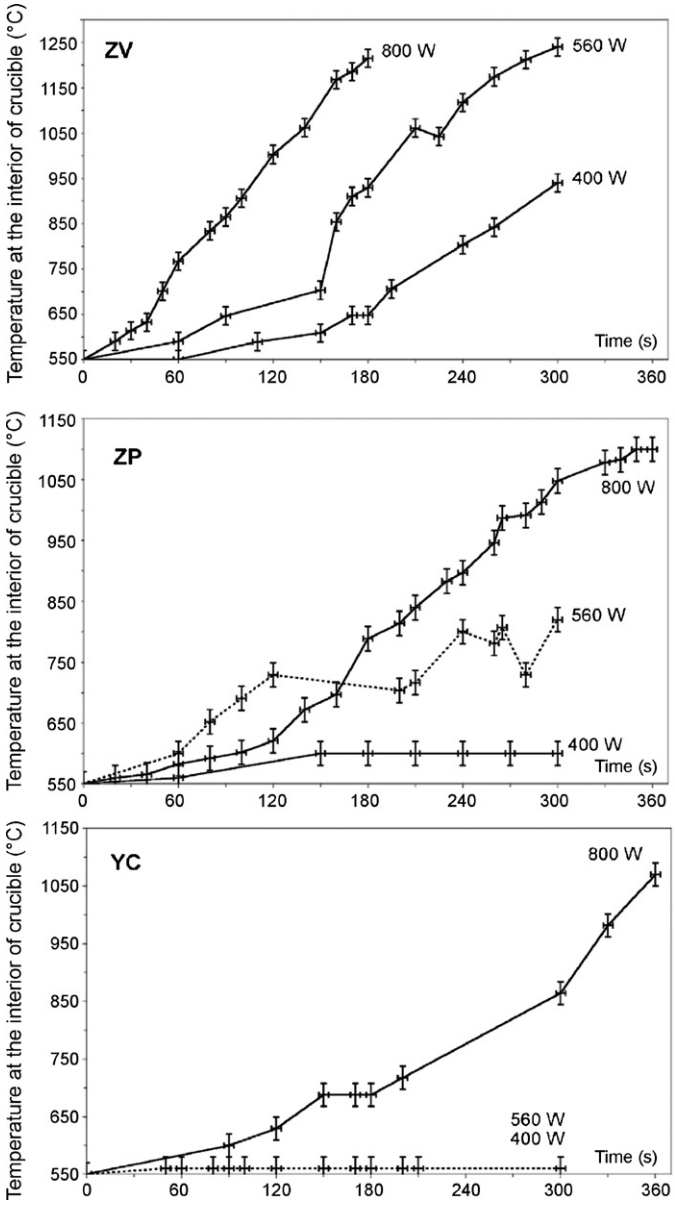

Fig. 4. Activation kinetics of the Cr:$YAlO_3$ (YC), Pr:$ZrSiO_4$ (ZP), and V:$ZrSiO_4$ (ZV) systems: inferred temperature at the interior of crucible in function of time at different MW power (pre-heating temperature: 700 °C).

promotes the $ZrO_2 + SiO_2 \rightarrow ZrSiO_4$ transformation; the new formed zircon would play an opposite role, being transparent to microwaves, so hampering the process by reducing the global tan δ value. The slow kinetics of the YC batch would be easily explained by the small amount of the only MW-active component (1.1 wt.% Cr) if Y_2O_3 was transparent to MW like Al_2O_3 is.

The reaction yield, intended as the weight percent of the desired phase, is affected by the pre-heating temperature in electric furnace (Fig. 5A). It can be appreciated that the YC system achieves a yield close to 100%, comparable to that of industrial manufacturing, despite its kinetics much slower than that of zircon pigments. The colour performance is good, with an optimum for a pre-heating temperature of 800 °C (Fig. 5B). The ZV pigment is the most sensitive to dielectric heating, being activated even at 300 °C, but its reaction yield remains low until the pre-heating temperature reaches 800 °C. As known also for the conventional heating,[26,27] the reactions occurring in the V_2O_5–SiO_2–ZrO_2 system are difficult to be accurately controlled. A microwave treatment beyond 6 min may result in overheating (temperature measured were up to 1500 °C) and melting. The ZP pigment exhibits a very low yield, even after pre-treatment in furnace at 1000 °C, although its colour performance is considerably improved starting from pre-heating to 800 °C. This low yield could be explained by the decreasing tan δ due to the $ZrO_2 + SiO_2 \rightarrow ZrSiO_4$ transformation.

The phase composition of pigments is summarized in Tables 1 and 2. Perovskite pigments synthesized by dielectric

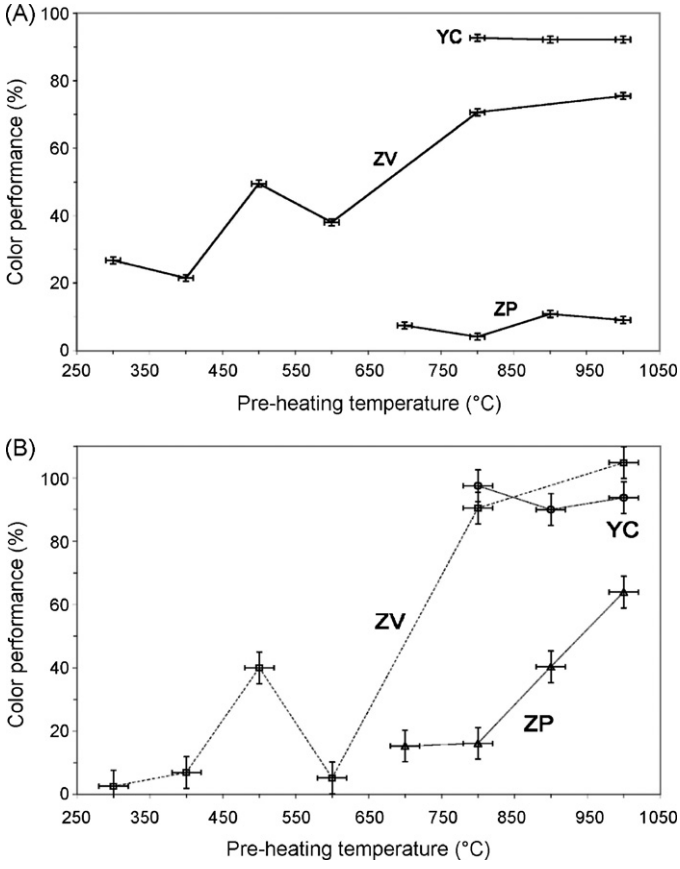

Fig. 5. Reaction yield (A) and colour performance (B) after MW irradiation (800 W, 5 min) in function of the pre-heating temperature in conventional electric furnace. Samples ZV pre-heated at 600 or 800 °C were irradiated for 3 min; pre-heated at 1000 °C for 1 min.

heating present only small differences with respect to Cr–$YAlO_3$ obtained by conventional firing: the amount of YAP is around 92% in all samples (~94% in the industrial pigment) while the unit cell parameters are very close to each other (Table 3). Accessory phases formed under MW irradiation are YAG ($Y_3Al_5O_{12}$, ~3 wt.%) and YAM ($Y_4Al_2O_9$, ~4.5 wt.%) instead of Y_2O_3, YOF and CaF_2, which were found in the YC system after conventional firing.[25] The occurrence of YAG and YAM is expected since they are thermodynamically favoured phases.[32] However, the absence of fluorides and oxyfluorides might suggest some volatilization of fluorine while removing the refractory lid to measure the T_{int} at the end of heating cycle or during the crucible transfer from electric furnace to MW oven.

In the ZV system, an increased $ZrSiO_4$-to-ZrO_2 ratio is observed for increasing pre-heating temperature (Table 2) which can explain the improved colour performance. The unit cell parameters of zircon vary in a rather restricted range over the whole interval of pre-heating temperature (Table 3) and allow an estimation of the actual vanadium content incorporated in the zircon lattice from literature data.[25,26,33,34] On this basis, the V amount seems to be approximately from 0.5 to 1.5 wt.% (Fig. 6). No secondary V-bearing phases were found, so vanadium probably underwent a volatilization, as known from industrial practice and literature.[27,35]

Phase composition of the ZP system exhibits just little changes even when the pre-heating temperature is raised from 700 to 1000 °C (Table 2). The $ZrO_2 + SiO_2 \rightarrow ZrSiO_4$ transformation rate is very low and no more than 11% of zircon is formed. Nevertheless, the unit cell parameters of zircon exhibit a significant growth with increasing pre-heating temperature (Table 3 and Fig. 6) which correspond to a parallel improvement of colour performance. This behaviour may be explained by a progressive incorporation of the larger Pr^{4+} ion (ionic radius 0.96 Å) in sub-

Table 1
Quantitative phase composition of YC ceramic pigment (wt.%).

Pre-heating temperature (°C)	Time of MW irradiation (min)	$YAlO_3$ (perovskite)	$Y_3Al_5O_{12}$ (YAG)	$Y_4Al_2O_9$ (YAM)
800	5	92.5	2.5	4.5
900	5	92.0	3.5	4.5
1000	5	92.0	3.0	5.0

Standard deviation of data is ±0.5%.

Table 2
Quantitative phase composition of ZP and ZV ceramic pigments (wt.%).

	Pre-heating temperature (°C)	Time of MW irradiation (min)	$ZrSiO_4$ (zircon)	ZrO_2 (baddeleyite)	SiO_2 (quartz)	SiO_2 (cristobalite)	SiO_2 (amorphous)
ZV	300	5	26.5	42.0	5.0	2.0	24.5
	400	5	21.5	45.5	2.0	0.0	31.0
	500	5	49.5	27.0	0.0	2.0	21.5
	600	3	38.0	34.5	0.0	3.5	23.5
	800	3	70.5	13.0	10.5	0.0	6.0
	1000	1	75.5	9.5	6.5	0.0	8.5
ZP	700	5	7.5	58.5	0.0	0.0	34.0
	800	5	4.0	60.5	0.0	0.0	35.0
	900	5	11.0	56.0	4.5	5.5	23.0
	1000	5	9.0	57.5	14.0	4.5	15.0

Standard deviation of data is ±0.5%.

Table 3
Unit cell parameters of zircon and perovskite pigments.

	Pre-heating temperature (°C)	Time of MW irradiation (min)	*a* (Å)	*b* (Å)	*c* (Å)	Volume (Å^3)
ZV	300	5	6.605	6.605	5.982	260.95
	400	5	6.603	6.603	5.980	260.76
	500	5	6.604	6.604	5.980	260.81
	600	3	6.602	6.602	5.980	260.69
	800	3	6.603	6.603	5.983	260.86
	1000	1	6.603	6.603	5.985	260.94
ZP	700	5	6.603	6.603	5.973	260.38
	800	5	6.602	6.602	5.977	260.50
	900	5	6.608	6.608	5.982	261.20
	1000	5	6.609	6.609	5.983	261.29
YC	800	5	5.326	7.375	5.183	203.59
	900	5	5.326	7.375	5.183	203.57
	1000	5	5.326	7.376	5.182	203.56
$YAl_{0.965}Cr_{0.035}O_3$ [28]			*5.332*	*7.377*	*5.184*	*203.91*

Standard deviation is ±1 in the last decimal figure.

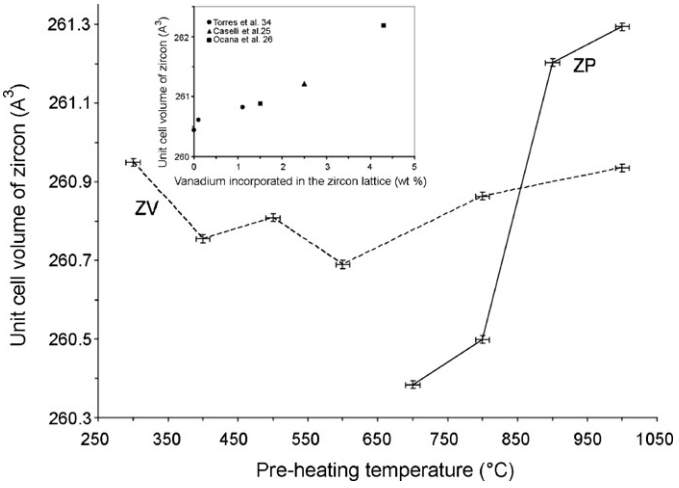

Fig. 6. Unit cell parameters of V–$ZrSiO_4$ (ZV) and Pr–$ZrSiO_4$ (ZP) pigments. Dependence of the unit cell volume of zircon on its vanadium content (inset).

stitution of Zr^{4+} (0.84 Å) in the 8-fold coordinated site of zircon lattice.[36,37] The remaining praseodymium ions were likely to be hosted in the ZrO_2 structure, since no transitory phases were found, like $Pr_2Zr_2O_7$ or $Na_2Pr_8Si_6O_{24}F_2$.[27,37]

In both zircon systems, the dielectric heating induced strong changes in silica phases: quartz, present in the starting batches, is partly preserved, partly transformed into cristobalite and to a large extent gave rise to an amorphous phase, which is more abundant after low temperature pre-heating. Such unexpected behaviour could be a peculiar effect of MW irradiation, fostering the mineralizer's amorphisation action on silica. This effect could be reduced at the higher pre-heating temperatures due to an experimental artefact: the partial volatilization of mineralizers during crucible transfer from electric furnace to MW oven.

4. Conclusions

The synthesis of ceramic pigments based on zirconium silicate and yttrium aluminium perovskite was accomplished for the first time through an innovative microwave-assisted two-step route. It consists of a short time pre-heating in conventional electric furnace then dielectric heating in MW oven for a few minutes, so being able to reduce dramatically the total synthesis time from many hours down to 5–10 min.

The V–$ZrSiO_4$ system is easily activated, already for a pre-heating temperature of 300 °C, but satisfactory reaction yield and colour performance are achieved only after pre-heating over 700 °C. Being highly sensitive to microwaves, this pigment is difficult to be kept under control, since temperatures over 1200 °C may occur even after a short time MW irradiation.

The dielectric heating of the Pr–$ZrSiO_4$ system is active only after pre-heating over 600 °C and proceeds with a slow kinetics, resulting in a low reaction yield. Nevertheless, the colour performance of pigments was rapidly improved at the higher pre-heating temperatures due to fostered incorporation of Pr ions into the zircon lattice.

Despite its difficult activation under dielectric heating, occurring only after pre-heating over 700 °C, the Cr–$YAlO_3$ pigment is formed with high reaction yield and good colour performance, practically the same of industrial pigments synthesized by conventional firing.

A peculiar effect of dielectric heating was observed in zircon pigments, consisting of silica amorphisation, even after low temperature pre-heating. There are clues that a partial volatilization of mineralizers occurred when pre-heating was carried out at higher temperatures, causing a reduced amorphisation of silica phases.

References

1. Rao, K. J., Vaidhyanathan, B., Ganguli, M. and Ramakrishnan, P. A., Synthesis of inorganic solids using microwaves. *Chem. Mater.*, 1999, **11**, 882–895.
2. Kasapoglu, N., Baykal, A., Koseoglu, Y. and Toprak, M. S., Microwave-assisted combustion synthesis of $CoFe_2O_4$ with urea, and its magnetic characterization. *Scripta Mater.*, 2007, **57**, 441–444.

3. Nayak, B. B., Vitta, S. and Bahadur, D., Synthesis and properties of nanograined La–Ca–manganite–Ni–ferrite composites. *Mater. Sci. Eng. B*, 2007, **139**, 171–176.
4. Wang, W. W., Zhu, Y. J. and Ruan, M. L., Microwave-assisted synthesis and magnetic property of magnetite and hematite nanoparticles. *J. Nanopart. Res.*, 2007, **9**, 419–426.
5. Bondioli, F., Corradi, A. B., Ferrari, A. M., Leonelli, C., Siligardi, C., Manfredini, T. *et al.*, Microwave synthesis of Al_2O_3/Cr_2O_3 (ss) ceramic pigments. *J. Microwave Power Electr. Energy*, 1998, **33**, 18–23.
6. Cherian, M., Rao, M. S., Manoharan, S. S., Pradhan, A. and Deo, G., Influence of the fuel used in the microwave synthesis of Cr_2O_3. *Top. Catal.*, 2002, **18**, 225–230.
7. Kimura, T., Takizawa, H., Uheda, K., Endo, T. and Shimada, M., Microwave synthesis of yttrium iron garnet powder. *J. Am. Ceram. Soc.*, 1998, **81**, 2961–2964.
8. Subasri, R., Mathews, T. and Sreedharan, O. M., Microwave assisted synthesis and sintering of $La_{0.8}Sr_{0.2}Ga_{0.83}Mg_{0.17}O_{2.815}$. *Mater. Lett.*, 2003, **57**, 1792–1797.
9. Malghe, Y. S., Gurjar, A. V. and Dharwadkar, S. R., Synthesis of $LaCoO_3$ from lanthanum trisoxalatocobaltate(III) (LTC) precursor employing microwave heating technique. *J. Therm. Anal. Calorim.*, 2004, **78**, 739–744.
10. Gao, W. Y., Sun, J. C., Liu, S., Liu, Y., Li, C. M. and Tang, N. L., Electrical properties and microwave synthesis of mixed rare earth oxide $Ln_{0.7}Sr_{0.3-x}Ca_xCo_{0.9}Fe_{0.1}O_{3-\delta}$. *J. Rare Earths*, 2006, **24**, 288–292.
11. Sacanell, J., Bellino, M. G., Lamas, D. G. and Leyva, A. G., Synthesis and characterization $La_{0.6}Sr_{0.4}CoO_3$ and $La_{0.6}Sr_{0.4}Co_{0.2}Fe_{0.8}O_3$ nanotubes for cathode of solid-oxide fuel cells. *Physica B*, 2007, **398**, 341–343.
12. Lagashetty, A., Havanoor, V., Basavaraja, S., Balaji, S. D. and Venkataraman, A., Microwave-assisted route for synthesis of nanosized metal oxides. *Sci. Technol. Adv. Mater.*, 2007, **6**, 484–493.
13. Subramanian, V., Burke, W. W., Zhu, H. W. and Wei, B. Q., Novel microwave synthesis of nanocrystalline SnO_2 and its electrochemical properties. *J. Phys. Chem. C*, 2008, **112**, 4550–4556.
14. Bilecka, I., Djerdj, I. and Niederberger, M., One-minute synthesis of crystalline binary and ternary metal oxide nanoparticles. *Chem. Commun.*, 2008, **7**, 886–888.
15. Katsuki, H. and Komarneni, S., Microwave-hydrothermal synthesis of monodispersed nanophase alpha-Fe_2O_3. *J. Am. Ceram. Soc.*, 2001, **84**, 2313–2317.
16. Kumari, L. S., George, G., Rao, P. P. and Reddy, M. L. P., The synthesis and characterization of environmentally benign praseodymium-doped $TiCeO_4$ pigments. *Dyes Pigments*, 2008, **77**, 427–431.
17. Tompsett, G. A., Curtis-Conner, W. and Sigfrid-Yngvesson, K., Microwave synthesis on nanoporous materials. *Chem. Phys. Chem.*, 2006, **7**, 296–319.
18. Celer, E. B. and Jaroniec, M., Temperature-programmed microwave-assisted synthesis of SBA-15 ordered mesoporous silica. *J. Am. Chem. Soc.*, 2006, **128**, 14408–14414.
19. Bondioli, F., Ferrari, A. M., Leonelli, C., Siligardi, C., Neil, A. H. and Evans, G., The application of microwaves in the synthesis of $Ce_{0.9}Pr_{0.1}O_2$ nanostructured powders. *J. Mater. Chem.*, 2005, **15**, 1061–1066.
20. Bondioli, F., Ferrari, A. M., Lusvarghi, L., Manfredini, T., Nannarone, S., Pasquali, L. *et al.*, Synthesis and characterization of praseodymium-doped ceria powders by a microwave-assisted hydrothermal (MH) route. *J. Mater. Chem.*, 2005, **15**, 1061–1066.
21. Calbo, J., Gargori, C., Sorlí, S., Badenes, J., Tena, M. A. and Monrós, G., Synthesis of ceramic pigments employing microwave radiation. *Bol. Soc. Esp. Ceram. Vidrio*, 2007, **46**, 14–20.
22. Bondioli, F., Leonelli, C., Manfredini, T., Ferrari, A. M., Caracoche, M. C., Rivas, P. C. *et al.*, Microwave-hydrothermal synthesis and hyperfine characterization of praseodymium-doped nanometric zirconia powders. *J. Am. Ceram. Soc.*, 2005, **88**, 633–638.
23. Suvorov, S. A., Turkin, I. A., Printsev, L. N. and Smirnov, A. V., Microwave synthesis of materials from aluminum oxide powders. *Refract. Ind. Ceram.*, 2000, **41**, 295–299.
24. Badenes, J. A., Vicent, J. B., Llusar, M., Tena, M. A. and Monrós, G., The nature of Pr–$ZrSiO_4$ yellow ceramic pigment. *J. Mater. Sci.*, 2002, **37**, 1413–1420.
25. Caselli, C., Lusvardi, G., Malavasi, G., Menabue, L. and Miselli, P., Multitechnique approach to V–$ZrSiO_4$ pigment characterization and synthesis optimization. *J. Eur. Ceram. Soc.*, 2007, **27**, 1743–1750.
26. Ocaña, M., Gonzalez-Elipe, A. R., Orera, V. M., Tartaj, P. and Serna, C. J., Spectroscopic studies on the localization of vanadium(IV) in vanadium-doped zircon pigments. *J. Am. Ceram. Soc.*, 1998, **81**, 395–400.
27. Llusar, M., Vicent, J. B., Badenes, J., Tena, M. A. and Monrós, G., Environmental optimisation of blue vanadium zircon ceramic pigment. *J. Eur. Ceram. Soc.*, 1999, **19**, 2647–2657.
28. Cruciani, G., Matteucci, F., Dondi, M., Baldi, G. and Barzanti, A., Structural variations of Cr-doped (Y,REE)AlO_3 perovskites. *Z. Kristallogr.*, 2005, **220**, 930–937.
29. Matteucci, F., Lepri Neto, C., Dondi, M., Cruciani, G., Baldi, G. and Boschi, A. O., Colour development of red perovskite pigment Y(Al,Cr)O_3 in various ceramic applications. *Adv. Appl. Ceram.*, 2006, **105**, 99–106.
30. Larson, A. C. and Von Dreele, R. B., General Structure Analysis System (GSAS). Los Alamos Nat. Lab. Report LAUR, 2000, pp. 86–748.
31. Toby, B. H., EXPGUI, a graphical user interface for GSAS. *J. Appl. Crystallogr.*, 2001, **34**, 210–213.
32. Fabrichnaya, O., Seifert, H. J., Ludwig, T., Aldinger, F. and Navrotsky, A., The assessment of thermodynamic parameters in the Al_2O_3–Y_2O_3 system and phase relations in the Y–Al–O system. *Scand. J. Metall.*, 2001, **30**, 175–183.
33. Ardizzone, S., Cappelletti, G., Fermo, P., Oliva, C., Scavini, M. and Scime, F., Structural and spectroscopic investigations of blue, vanadium-doped $ZrSiO_4$ pigments prepared by a sol–gel route. *J. Phys. Chem. B*, 2005, **109**, 22112–22119.
34. Torres, F. J., Tena, M. A. and Alarcon, J., Rietveld refinement study of vanadium distribution in V^{+4}–$ZrSiO_4$ solid solutions obtained from gels. *J. Eur. Ceram. Soc.*, 2002, **22**, 1991–1994.
35. Alarcon, J., Crystallization behaviour and microstructural development in $ZrSiO_4$ and V–$ZrSiO_4$ solid solutions from colloidal gels. *J. Eur. Ceram. Soc.*, 2000, **20**, 1749–1758.
36. Del Nero, G., Cappelletti, G., Ardizzone, S., Fermo, P. and Gilardoni, S., Yellow Pr–zircon pigments—the role of praseodymium and of the mineralizer. *J. Eur. Ceram. Soc.*, 2004, **24**, 3603–3611.
37. Ocaña, M., Caballero, A., Gonzalez-Elipe, A. R., Tartaj, P., Serna, C. J. and Merino, R. I., The effects of the NaF flux on the oxidation state and localisation of praseodymium in Pr-doped zircon pigments. *J. Eur. Ceram. Soc.*, 1999, **19**, 641–648.